

Dasatinib and Hesperidin Loaded Nano Formulation and Preclinical Evaluation for Anticancer Activity

Moinuddin¹, Sachin Neekhara,² SK Swarnkar,^{3*} Puneet Gupta,³ Deepa Gupta,³ Alok Khunteta,³ Ujjwal Kaushik,⁴ Saeem Ahmad⁵

¹Dabur Research Foundation, Ghaziabad, Uttar Pradesh, India.

²Department of Pharmacy, Maharishi University of Information Technology, Lucknow, Uttar Pradesh, India.

³Lal Bahadur Shastri College of Pharmacy, Jaipur, Rajasthan, India.

⁴Chitkara College of Pharmacy, Chitkara University, Rajpura, Punjab, India.

⁵Jamia Hamdard, New Delhi, India.

Received: 13th March, 2023; Revised: 18th July, 2023; Accepted: 22th August, 2023; Available Online: 25th September, 2023

ABSTRACT

In this study, we aimed to develop Dasatinib/hesperidin-loaded-SLNs for chronic myeloid leukemia (CML). Utilizing a high-shear homogenizer for the synthesis, “central composite design (CCD)” was used to enhance the dasatinib/hesperidin loaded-SLNs. The optimized SLNs had PDI, particle size, and average entrapment efficiency of 0.12%, 162.3 nm, and 93%, respectively. Therefore, by enhancing the total amount of Compritol as well as sonication time the polydispersity was increased. Poloxamer 188 content had a significant influence in decreasing the polydispersity index and the entrapment efficiency (EE) of the SLN was found to be 93%. Through TEM, SEM, FTIR, DSC, and HPLC analysis, SLNs were characterized, and their anticancer efficiency was assessed in both *in-vitro* and *in-vitro* cell viability tests (MTT). SLNs containing dasatinib and hesperidin have rounded and spherical shape having a diameter of 200 nm. DSC and FTIR tests showed compatibility between the drugs and excipients. The drug release from optimized SLN formulation was under observation for 48 hours. It was found that the medication released its drug components over a protracted period of time, with 30% of the drug being released in the first four hours and the remainder 76% in the next 48 hours. According to the IC₅₀ values determined by an independent study, dasatinib, hesperidin, and SLN were 33.97, 5158, and 4.03 µg/mL, respectively. A comparison of SLN and free drugs revealed that SLN was more effective at cytotoxicity. In this study, dasatinib and hesperidin-loaded SLNs for chronic myeloid leukemia (CML) against HL60 human leukemia cell lines were prepared and evaluated using a novel formulation approach free of toxic excipients.

Keywords: Chronic myeloid leukaemia (CML), Dasatinib, HL60 human leukemia cell lines, Hesperidin, Oral bioavailability, SLN.

International Journal of Pharmaceutical Quality Assurance (2023); DOI: 10.25258/ijpqa.14.3.20

How to cite this article: Moinuddin, Neekhara S, Swarnkar SK, Gupta P, Gupta D, Khunteta A, Kaushik U, Ahmad S. Dasatinib and Hesperidin Loaded Nano Formulation and Preclinical Evaluation for Anticancer Activity. International Journal of Pharmaceutical Quality Assurance. 2023;14(3):579-586.

Source of support: Nil.

Conflict of interest: None

INTRODUCTION

The myeloproliferative neoplasm (MPN) is referred to as chronic myeloid leukemia (CML) and found to have an incidence of^{1,2} cases per 1,00000 individuals.^{1,2} It is characterized by mutations to the hematopoietic system as well as lower production of healthy hematopoietic cells. These mutations cause the cells to proliferate or accumulate by preventing cell differentiation. About 50% of CML patients in the US are asymptomatic, and they are often diagnosed by normal medical examinations or testing.³ Three phases of CML can be distinguished: the accelerated phase (AP),

the chronic phase (CP), and the blast phase (BP).⁴ Advances in targeted therapies via selective protein kinase inhibitors have shown a significant impact on the treatment of various human malignancies, in which these agents prompt major clinical responses with significantly fewer adverse effects than conventional cytotoxic chemotherapy.^{5,6} As a result, prognostic stratification and treatment options have been improved. Thus, novel targeted therapies for CML have recently received major attention.⁷⁻⁹ A broad range of applications in the biomedical area have been made possible by the capacity to generate

*Author for Correspondence: skswarnkar@gmail.com

nanoparticles that are in the same size range as proteins. These particles may stimulate, react with, and impact target cells and tissues to assure the intended physiological reactions while reducing unwanted outcomes.^{4,6}

Dasatinib is a second-generation tyrosine kinase inhibitor (TKI) that is taken orally and has antiproliferative activity against CML.¹⁰ In the case of resistance to imatinib, it can also be used as an alternative to imatinib therapy. The action of dasatinib is 325 times more efficient than that of imatinib against unmutated BCR-ABL, and it has antagonistic effects against most imatinib-resistant mutants of BCR-ABL, and survival of cancer cells and reducing vascular permeability.¹¹⁻¹³ On the other hand, drawbacks of dasatinib are reported such as pH-dependent solubility (205 g/mL at pH 4.27 and < 1 g/mL at pH 6.98), poor absorption, and significant first-pass effect, which results in oral bioavailability of only 14–34%.^{14,15} Furthermore, particular individuals may be at risk of experiencing therapeutically relevant toxicity due to the increased of dasatinib dose.¹³ Hence, new nanoformulations of dasatinib are required for improved oral bioavailability.

Studies have shown that consuming flavonoid-rich diets prevents several chronic diseases and cancer, resulting in consuming flavonoid-rich supplements to treat cancer.¹⁶ Due to the steadily rising global frequency of malignancies, there is an urgent need for innovative, effective medicines and treatment techniques.¹⁷ Hesperidin, a nontoxic natural substance that exhibits potent anticancer activities, may provide new therapeutic options for cancer patients. In multiple preclinical studies, it has been demonstrated that it protects against malignant transformation and progression.^{18,19} Hesperidin can alter tumor cell survival, division, and death mechanisms. Nevertheless, hesperidin does not have wide clinical use due to its decreased solubility in water.²⁰ Researchers are focusing on overcoming this problem by developing appropriate delivery systems for hesperidin.

A monolayer surfactant shell surrounds an important solid lipid core in solid lipid nanoparticles (SLNs). In comparison, SLNs were found to be a safer option than other nanosystems.²¹ They often avoid significant difficulties, such as liposomes' poor durability, decreased loading capacity, potentially high biotoxicity, and residual organic solvent when using polymeric nanoparticles.²² It has been demonstrated that SLN's lipidic components can solubilize highly lipophilic pharmaceuticals, which has the benefit of keeping SLNs in a more stable solution, without need for significant much surfactants and enhancing biopharmaceutical performance following various administration methods. Furthermore, SLNs make the drugs targeted to the lymphatic system, which has a variety of advantages such as protection from hepatic first-pass metabolism, enhanced drug bioavailability, and reduced hepatotoxicity.²³

With the use of a high-shear homogenizer, we especially planned to create stable dasatinib and hesperidin-loaded SLNs for CML in this work. As far as we know, no earlier studies have discussed using co-loaded nanocarriers in this way.

MATERIALS AND METHODS

The precirol ATO and Compritol were purchased from Gattetosse (Saint-Priest, France), Poloxamer 188 was purchased from CDH (New Delhi, India), hesperidin was purchased from Wuhan amino acid biochemicals (Wuhan, China), and Dasatinib was procured from Dr. Reddy's Laboratory Ltd (Hyderabad, India). Analytical quality (HPLC grade) materials were employed for the study.

Preparation of SLN

SLN was prepared using the high-shear homogenizer method. Briefly, 0.2 to 1.5% (w/v) Compritol-188 was melted at 50°C (oil phase). The oil phase was mixed with dasatinib and hesperidin for about 15 minutes while agitated at 600 rpm using a magnetic stirrer. The obtained emulsion was injected into a 100 mL aqueous solution containing 5% (w/w) poloxamer 188 while being homogenized (IKA T 25D, Germany) for 10 minutes duration at 20k rpm followed by sonication using a probe sonicator to obtain the desired nanoscale.^{10,24-27}

Design of Experiment for the Optimization of SLN

The Design Expert® program, version 13 was utilized to improve the dasatinib/hesperidin-loaded SLN by central composite design (CCD).

The experimental design for formulation development is the fundamental factor for constructing the preliminary screening of the experiment. To decrease the number of runs with 3/4 variables, a twenty-run, 3-factor, 3-level 'CCD' was used for process optimization. The quadratic response surface as well as constricting second-order polynomials, were examined using software. Using the replicated center point and a set of midpoints of the edge of a multi-dimensional cube, this well-defined region of interest. This allowed us to assess main effects and interactions of the formulation ingredients used and permit us to optimize the formulation.²⁸ Based on the design, a linear quadratic model was produced, as shown in Table 1.

Experimental Data Analysis Using Design Expert®

Experiment results were analyzed using Design Expert software (13th), providing valuable information, and reinforcing statistical design's utility. Table 2 shows the effects of compritol,

Table 1 CCD variables- actual levels and constraints.

<i>Factors</i>	<i>Coded Levels</i>		
Independent variable	Low (-1)	Medium (0)	high(+1)
X1= Campritol (%)	0.2	0.85	1.5
X2= Poloxamer (%)	1	3	5
X3= Time in minutes for Sonication	1	5.5	10
Dependent variables	Constraints		
Y1= Size of Particle(nm)	(100–200)		
Y2= Polydispersity Index (PDI)	Minimum		
Y3= Average Efficiency of Entrapment (%)	Maximum		

Poloxamer 188, and sonication duration on the polydispersity index (PDI), particle size, and entrapment efficiency.²⁹

By using Design-Expert Software's estimated statistical parameters, such as the modified multiple coefficient, anticipated residual sum of squares, and multiple correlation coefficient, polynomial equations, including important cause-and-effect variables, were created. Using ANOVA provision in the software, we validated the polynomial equation statistically.

Physical Characterization of SLN

Suitable dilutions of nanodispersion were performed with water for zeta potential, size determination, and PDI measurement at $25 \pm 1^\circ\text{C}$ using Nano ZS.³⁰

Morphology Studies

Transmission electron microscopy (TEM)

The optimized SLN was diluted 10 times with Milli Q water before placing a drop of sample of SLN solution onto the cu-grid and allowed to dry at room temperature. It was then stained with 1% phosphotungstic acid for better visibility, and the TEM photomicrographs were taken with the ((TEM) (Tecnai G2 S-twin, FEI, Netherland) instrument.³¹

Scanning electron microscopy (SEM)

The optimized sample solution was used for SEM photomicrographs and captured at 10Kv.³²

Physiochemical Characterization

Fourier transform infrared spectrophotometric analysis

To investigate the drug-polymer interactions, an appropriate number of samples were analyzed, and the %transmittance was recorded using the FTIR (FTIR, Nicolet iS5) instrument in a scanned range of 400 to 4000 cm^{-1} .³³

Differential scanning calorimetry (DSC) analysis

Five milligrams (5 mg) of drug sample were accurately weighed & put in the hermetically sealed aluminum (Al) DSC pan. Further, the pan was sealed using hydraulic press. The sample was scanned within the temp. range of 40 to 400°C with given (10°C/min) heating rate. This study was executed using the DSC, model DSC6 instrument.

HPLC analysis

The hesperidin and dasatinib concentrations were determined using RP-HPLC with the zorbax eclipse xdb C-8 column with 1.0 mL/min flow rate at 30°C. The mobile phase was a mixture of methanol and phosphate buffer (2.75 g potassium dihydrogen phosphate KH_2PO_4 in 1000 mL milli-Q water) (48:52) & the pH was adjusted to 4.5. After 15 minutes, the 10 μL sample was injected and scanned at 280 and 323 nm.^{34,35}

Preparation of standard

1000 ppm solution was prepared with DMSO. For further dilution methanol was used. Vortexed and sonicated for 10 minutes each, filtered.

Preparation of sample

Added 1-mL of DMSO to 500 mg of sample in a 2 mL Eppendorf tube. As previously mentioned, vortex, sonicate,

and centrifuge for 10 minutes at 14000 rpm. Next, add another 1-mL of DMSO to 1-mL of the supernatant layer. The same procedures were used for centrifuging, sonicating, and vortexing. injected the filtered upper layer into the HPLC after taking it.³⁶

Encapsulation efficiency

In 1-mL of DMSO was added to 500 mg of the sample in a 2 mL eppendorf tube. Centrifuge the sample solution for 10 minutes followed by a vortex and sonication. Then took the supernatant layer of about 1-mL and added 1-mL of H_2O . Followed the same for vortexing, sonication, and centrifuging. Took the upper layer, filter it, and injected it onto HPLC for analysis.

In-vitro drug release

After 24 hours of production under sink circumstances, the *in-vitro* drug release was evaluated as per the method discussed by Mühlen *et al.* (1998) and evaluated by HPLC after the various time intervals of 0, 0.25, 0.5, 1, 2, 4, 6, 8, and 12 hours.³⁷

MTT assay

In order to examine the cytotoxic capability of dasatinib and hesperidin-loaded solid lipid nanoparticles, cell viability assay utilizing the HL60 human leukemia cell line was performed. A 96-well flat-bottom microtiter plate with 1104 cells per well was seeded with cells and cultured for 36 hours to allow the cells to proliferate and adhere.³⁸ Afterward, dasatinib and hesperidin-loaded solid lipid nanoparticles were added at different concentrations (50 μg to 0.1 $\mu\text{g}/\text{mL}$) and incubated for 36 hours. Fresh media was added after 36 hours, and then for an additional 4 hours, the cells were incubated at 37°C with 20 μL of "3-(4,5-dimethylthiazol-2-yl)-2,5-diphenyl-2H-tetrazolium bromide" (MTT) (5 mg/mL in PBS). Additionally, DMSO, used to dissolve the Formazan crystals produced by the mitochondrial reduction of MTT. The computation was done by monitoring the absorbance at 540 nm using microplate reader (Mark-Bio-Rad), results were calculated using following equation.³⁹

$$\%Viable\ cells = [(Abs_{sample} - Abs_{blank}) / (Abs_{control} - Abs_{blank})] \times 100$$

RESULT AND DISCUSSION

Preparation of SLN by CCD Approach

In 20 experimental runs, 3 levels of central composite design were employed to build the polynomial models for optimization of formulation as mentioned in Table 2.⁴⁰⁻⁴³

Physical Characterization of SLN

Effect of the variable on particle size (Y_1)

As per the experiment results, particle size ranged from 145 to 265 as shown in Table 2. The amount of Compritol had an effect on the size. Following mentioned equation can elaborate effect of factor levels on particle size:

$$\text{Particle Size (Y1)} + 179.74.60 = 19.11A + 5.75B - 1.47C + 22.68AB + 3.00AC + 0.377BC - 8.21A^2 - 7.41B^2 - 14.84C^2$$

The primary effects of Y_1 through Y_3 reflect the average outcome of changing one variable at a time from one level to

another. The positive coefficients indicate that size is positively impacted. In contrast, negative coefficients before independent variables signify an unfavorable impact on size. Investigating these mentioned coefficients in the above 2nd order polynomial mode is shown in Figure 1(i) graph.

Moreover, model F-value for full quadratic particle size of nanoparticles was 20.69, indicating the linear response surface and quadratic model was significant as mentioned in Table 3. By analyzing responses surfaces predicted particle size as shown in Figure 1 (a) that an increase in Poloxamer 188 leads to a decrease in particle size.⁴⁴

Effect of the variable on poly dispersity index (Y2)

As per the obtained results from the experiments, the particle size value varies from PDI 0.125 to 0.934 as mentioned in Table 2. The small value of PDI was highly desirable to have even size distribution in the dispersion media. PDI was influenced by the amount of compritol and sonication time. Below mentioned equation shows the relationship between the above mention factors & PDI.

$$\text{Poly Dispersity Index (Y2)} +0.3575= -0.0822A-0.1693B-0.0040C+0.1524AB+0.0894AC+0.0004BC-0.0581A^2+0.3830B^2-0.1594C^2$$

The “Model F-value” of 14.00 implies the model is significant as mentioned in Table 3. A “Model F-value” this

Table: 2 Composition of 3 factors, 3 levels CCD for the formulation development

Run	A: Solid Lipid % (w/w)	B: Surf actant % (w/w)	C: Sonication Time (min)	Response 1 Particle Size	Response 2 PDI	Response 3 %EE
1	0.85	3	5.5	162.3	0.125	93
2	0.85	3	5.5	162.3	0.125	93
3	1.5	3	5.5	233	0.631	71
4	0.85	5	5.5	162.3	0.125	93
5	0.2	3	5.5	198	0.345	85
6	0.85	3	1	145	0.456	91
7	0.85	1	5.5	152	0.378	92
8	0.85	3	5.5	162.3	0.125	93
9	1.5	5	1	264	0.561	72
10	0.85	3	10	179	0.621	79
11	0.2	1	1	153	0.561	87
12	0.2	5	1	189	0.521	83
13	0.2	5	10	167	0.815	58
14	1.5	1	10	189	0.767	76
15	1.5	1	1	167	0.614	67
16	0.85	3	5.5	189	0.125	93
17	0.2	1	10	156	0.843	88
18	0.85	3	5.5	162.3	0.125	93
19	0.85	3	5.5	162.3	0.125	93
20	1.5	5	10	265	0.934	68

larger could only happen owing to noise with a 0.05% chance. Figure 1 (ii) showed the influence of different variables on PDI. The polydispersity increased as compritol and sonication duration were increased. The presence of poloxamer 188 significantly lowered the PDI.

Effect on encapsulation efficiency (Y3)

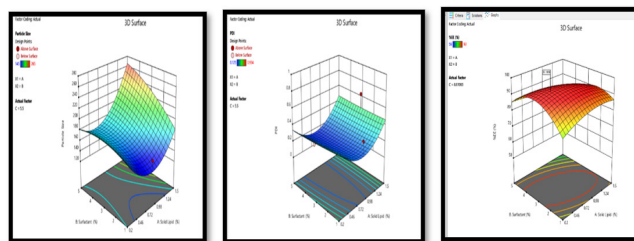
Encapsulation efficiency (EE) will demonstrate the preparative efficiency of compritol formulation. For EE, *p-values* of X₁ (Compritol), X₂ (Poloxamer 188), and X₃ (Sonication time) were all < 0.0001, signifying that these variables had noteworthy differences in the EE response as mentioned in Table 3. Encapsulation efficiency might get reduced with higher compritol concentration & lesser quantity of Cholesterol + Stearic acid. The following equation shows the relationship between the above-mentioned factors and encapsulation efficiency.⁴⁰

$$\text{Encapsulation Efficiency (Y3)} +88.2= 3.18A-3.60B+5.61C-5.25AB-7.00AC+1.25BC-3.80A^2-10.57B^2-5.49C^2$$

The model was vital, as indicated by the “Model F-value”

Table 3: Quadratic ANOVA model: results

Response	F-value	p-value	Mean square	Adjusted R2	Predicted R2	Remarks
Particle size (Y1)	20.69	<0.0001	2455.77	0.9032	0.6102	Significant
PolyDispersity Index (Y2)	14.00	<0.0001	0.1540	0.8603	0.4838	Significant
Encapsulation Efficiency (Y3)	22.35	<0.0001	245.87	0.9100	0.5098	Significant



(i) particle size (ii) Poly Dispersity Index (iii) Encapsulation Efficiency

Figure: 1 Response surface plots of (i) Particle size, (ii) Poly Dispersity Index, and (iii) Encapsulation Efficiency

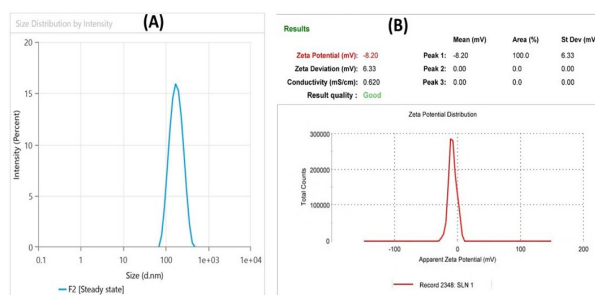


Figure 2: (A) Dasatinib-hesperidin SLN particle size and (B) Zeta potential after

of 8.53. The likelihood that a “Model F-value” would be this high owing to noise was 0.15% at most. Figure 1 shows the impact of several variables on the success of trapping (iii). The entrapment efficiency was decreased by enhancing the quantity of Compritol & sonication time. Surfactant contents did not have a significant influence in increasing the entrapment efficiency.

All formulations had PDI values between 0.125 and 0.934 with particle sizes varies from 145 to 265 nm (Table 2). Figures 1 and 2 illustrates the particle size range for this optimized formulation, which ranged from 162.3 to 0.12 nm.

Morphology Studies

In order to analyze the morphology of dasatinib and hesperidin-loaded SLN, scanning electron microscopy (SEM) and transmission electron microscopy (TEM) were used. (Figure 3)

Physiochemical Characterization

FTIR analysis

FTIR spectrum the drugs (dasatinib & hesperidin), and a mixture of drugs are shown in Figure 4. Other IR spectra of dasatinib-exciipients mixtures are shown in Figure 5 and IR spectra of hesperidin-exciipients mixtures are shown in Figure 6 and the final spectra of SLN formulation is shown in Figure 7.

Differential scanning calorimetry (DSC) analysis

The endotherm of dasatinib, hesperidin, and optimized SLN and their typical curve is shown in Figure 8. The absence of dasatinib and hesperidin peaks in optimized SLN formulation indicates that the drug was successfully loaded in the lipid core.

HPLC analysis

The calibration curve for dasatinib and hesperidin was constructed by plotting the concentration versus peak area.

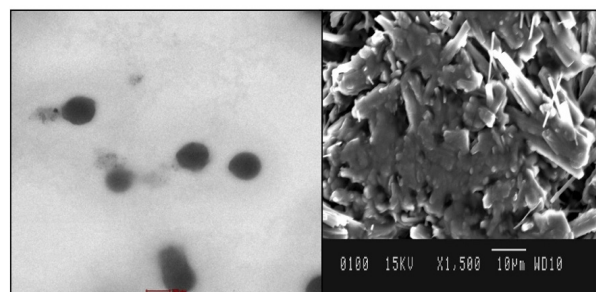


Figure 3: SEM and TEM analysis

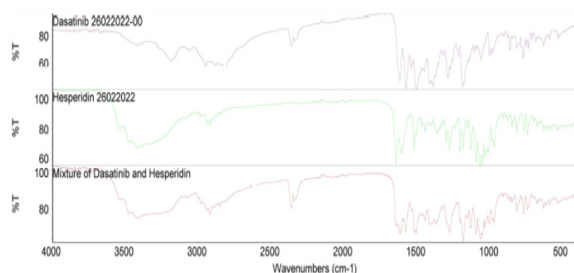


Figure 4: FTIR spectrum of dasatinib, hesperidin, and mixtures

The response was a linear function of dasatinib concentration in the range 25 to 300 µg/mL. The calibration plot’s regression equations were determined at a detection wavelength of 323 nm (Table 4, Figure 9). No major difference was observed between the slopes of calibration plots as mentioned in the integrated results(Figure 10).⁴⁵

Drug Release *in-vitro*

Releasing pattern of the SLN formulation and the suspension is shown in Figure 11. The results showed that for dasatinib and hesperidin, 45.5 and 31.4% of the drugs were released from the SLN in the first 4 hours, respectively, while 66.5 and 51.8% of the drugs were released in the concluding 24 hours. Results demonstrated a rapid drug release of substances adsorbed on the SLNs’ surface, followed by a ‘sustained release’ of the same substances, demonstrating that the substances were encapsulated in the ‘lipid core’. *In-vitro* drug release profile data was fitted to Higuchi square root (R^2 0.6624), Hixon–

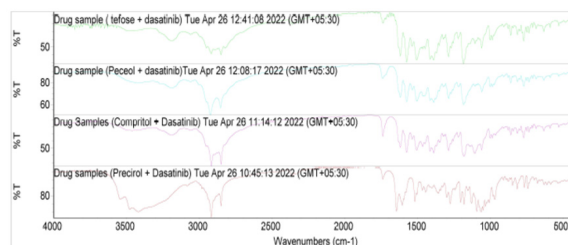


Figure 5: FTIR spectrum of dsatinib and excipients

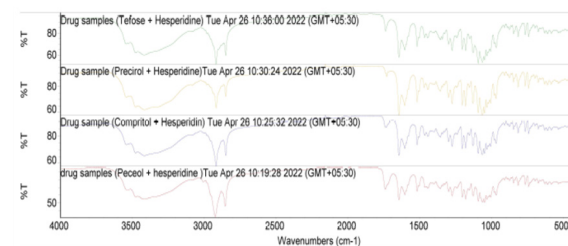


Figure 6: FTIR spectrum of hesperidin and excipients

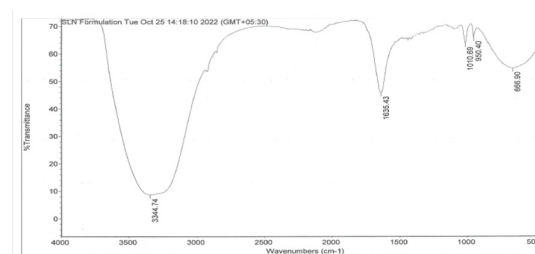


Figure 7: FTIR spectrum of SLN

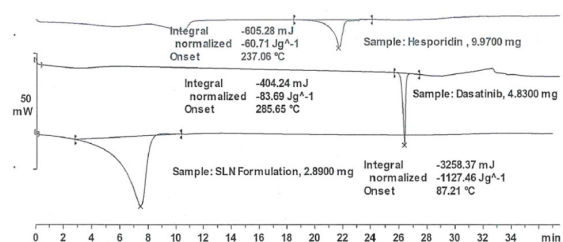


Figure 8: DSC analysis

Table 4: Linear regression data for dasatinib and hesperidin calibration curves

Conc. of dasatinib (mg/L)	Peak area (Y)	Conc. of hesperidin (mg/L)	Peak area (Y)
24.95	20.294	25.00	5.967
49.90	37.408	50.00	10.689
99.80	74.752	100.00	21.723
199.60	146.665	200.00	42.120
249.50	187.316	250.00	53.732
299.40	225.537	300.00	65.778
Intercept (a)	0.36	Intercept (a)	0.04
Slope (b)	0.75	Slope (b)	0.22
R	0.99983	R	0.99957
Equation	$y = 0.7457x + 0.3610$	Equation	$y = 0.22x + 0.04$

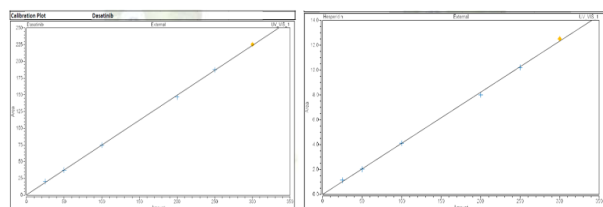


Figure 9: Typical HPLC chromatogram of dasatinib using a UV-visible detector at 323 nm

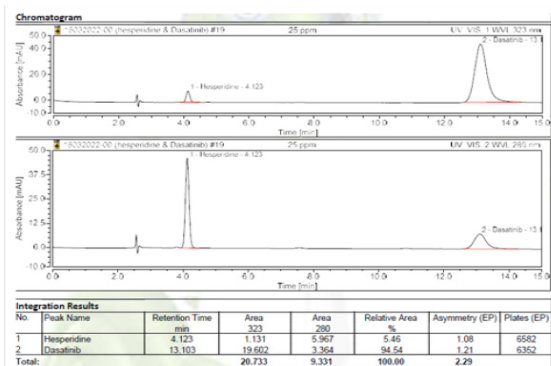


Figure 10: Integrated results

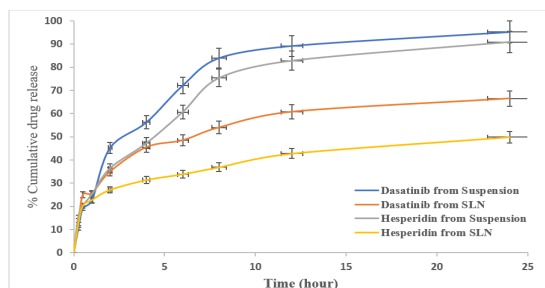


Figure 11. Release profiles of dasatinib and hesperidin from suspension and SLN formulations, *in-vitro*

Crowell cube root (R^2 0.7642), Korsmeyer–Peppas (R^2 0.9909) zero-order (R^2 0.6624) and first-order (R^2 0.6624) kinetic models. The Korsmeyer–Peppas model (highest R^2) provided a comprehensive explanation for the kinetic modeling of drug release from the improved SLN formulation.⁴⁶

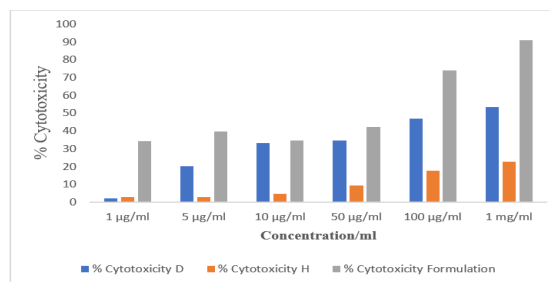


Figure 12: In-vitro cytotoxicity of Dasatinib & Hesperidin and optimized SLN formulation

In-vitro cell viability assay (MTT assay)

As shown in Figure 12, free dasatinib and hesperidin and optimized SLN formulation showed comparable cytotoxicity outcomes against HL60 human leukemia cell lines. According to the IC_{50} values determined by an independent study, dasatinib, hesperidin, and SLN were 33.97, 5158, and 4.03 $\mu\text{g/mL}$, respectively. A comparison of SLN and free drugs revealed that SLN was more effective at cytotoxicity.

CONCLUSION

In this study, we demonstrate that high-shear homogenizers are effective for preparing SLNs containing dasatinib & hesperidin for CML, which enhances the cytotoxicity and stability of dasatinib and hesperidin while reducing the associated toxic effects. The optimized formulation showed a narrow size distribution with a PDI of 0.12 and a particle size in the range of 162.3 nm based on the 20 run trials. In addition, they were able to release both dasatinib and hesperidin sustainably, demonstrating that the drugs were encapsulated in the lipid core. There was a 93% EE for the SLN. Each of the 3 variables X_1 (Comprititol), X_2 (Poloxamer 188), and X_3 (Sonication time) had a *p-value* equivalent to less than 0.0001, suggesting significant differences in particle size, PDI, and EE%. Dasatinib and hesperidin-loaded SLN’s TEM and SEM investigation indicated a spherical, round, and physically compatible form with a diameter of 200 nm. HL60 cells showed comparable cytotoxicity against dasatinib and hesperidin when combined with the optimized SLN formulation. A study conducted independently determined the IC_{50} values for dwasatinib, hesperidin, and SLN as 33.97, 5158, and 4.03 g/mL, respectively. A comparison of SLN and free drugs revealed that SLN was more effective at cytotoxicity. Therefore, the developed dual-targeted dasatinib and hesperidin demonstrated higher sensitivity of cells to the drug entrapped in SLN than the drug solution. As a result of the creation of sustained-release anticancer medication formulations, this unique method could lead to an improved prognosis and an increase in the quality of life for patients.

ACKNOWLEDGMENT

The authors acknowledge Dabur Research Foundation, Ghaziabad and Maharishi University of Information Technology, Lucknow, India for jointly providing opportunities to work at their facilities.

REFERENCES

- Htun HL, Lian W, Wong J, Tan EJ, Foo LL, Ong KH, et al. Classic myeloproliferative neoplasms in Singapore: A population-based study on incidence, trends, and survival from 1968 to 2017. *Cancer Epidemiol.* 2022;79:102175. Available from: DOI: <https://doi.org/10.1016/j.canep.2022.102175>
- Katogiannis K, Ikonomidis I, Panou F, Katsimardos A, Divane A, Tsantes A, et al. Leukostasis-Related Fatal Cardiopulmonary Arrest as Initial Chronic Myeloid Leukemia Presentation. *J Med Cases.* 2018;9(3):77–82. Available from: DOI: <https://doi.org/10.14740/jmc2993w>
- Jabbour E, Kantarjian H. Chronic myeloid leukemia: 2018 update on diagnosis, therapy and monitoring. *Am J Hematol.* 2018;93(3):442–59. Available from: DOI: <https://doi.org/10.1002/ajh.25011>
- Jabbour E, Kantarjian H. Chronic myeloid leukemia: 2020 update on diagnosis, therapy and monitoring. *Am J Hematol.* 2020;95(6):691–709. Available from: DOI: <https://doi.org/10.1002/ajh.25792>
- Vanneman M, Dranoff G. Combining immunotherapy and targeted therapies in cancer treatment. *Nat Rev Cancer.* 2012;12(4):237–51.
- Smyth LA, Collins I. Measuring and interpreting the selectivity of protein kinase inhibitors. *J Chem Biol.* 2009;2(3):131–51.
- Hu J, Xing K, Zhang Y, Liu M, Wang Z. Global Research Trends in Tyrosine Kinase Inhibitors: Coword and Visualization Study. *JMIR Med Inform.* 2022;10(4):1–18.
- Lopina N, Dmytrenko I, Hamov D, Lopin D, Dyagil I. A New Paradigm of Cardio-Hematological Monitoring in Chronic Myeloid Leukemia Patients Treated With Tyrosine Kinase Inhibitors. *Cureus.* 2022;14(6):5–14. Available from: DOI: <https://doi.org/10.7759/cureus.25766>
- Jim HSL, Hyland KA, Nelson AM, Pinilla-Ibarz J, Sweet K, Gielissen M, et al. Internet-assisted cognitive behavioral intervention for targeted therapy-related fatigue in chronic myeloid leukemia: Results from a pilot randomized trial. *Cancer.* 2020;126(1):174–80. Available from: DOI: <https://doi.org/10.1002/ncr.32521>
- Bhattacharya T, Soares GABE, Chopra H, et al. Applications of Phyto-Nanotechnology for the Treatment of Neurodegenerative Disorders. *Materials (Basel).* 2022;15(3):804. Available from: DOI: <https://doi.org/10.3390/ma15030804>.
- Yang SX, Dancey JE. *Handbook of Therapeutic Biomarkers in Cancer.* 2nd Editio. New York: Jenny Stanford Publishing; 2021. Available from: DOI: <https://doi.org/10.1201/9781003159469>
- Wolfe HR, Rein LAM. The Evolving Landscape of Frontline Therapy in Chronic Phase Chronic Myeloid Leukemia (CML). *Curr Hematol Malig Rep.* 2021;16:448–54. Available from: DOI: <https://doi.org/10.1007/s11899-021-00655-z>
- He S, Bian J, Shao Q, Zhang Y, Hao X, Luo X, et al. Therapeutic Drug Monitoring and Individualized Medicine of Dasatinib: Focus on Clinical Pharmacokinetics and Pharmacodynamics. *Front Pharmacol.* 2021;12(December):1–11. Available from: DOI: <https://doi.org/10.3389/fphar.2021.797881>
- Arafath AAMY, Jaykar B. Determining the Enhancement of Oral Bioavailability via Solid Lipid Nanoparticles of Anticancer Drug Dasatinib - An In-vitro Cytotoxicity and Pharmacokinetic Study. *Curr Asp Pharm Res Dev.* 2021;2:161–8. Available from: DOI: <https://doi.org/10.22159/ajpcr.2019.v12i6.33135>
- Dharani S, Mohamed EM, Khuroo T, Rahman Z, Khan MA. Formulation Characterization and Pharmacokinetic Evaluation of Amorphous Solid Dispersions of Dasatinib. *Pharmaceutics.* 2022;14(11):2450. Available from: DOI: <https://doi.org/10.3390/pharmaceutics14112450>
- Janabi AHW, Kamboh AA, Saeed M, Xiaoyu L, BiBi J, Majeed F, et al. Flavonoid-rich foods (FRF): A promising nutraceutical approach against lifespan-shortening diseases. *Iran J Basic Med Sci.* 2020;23(2):140–53. Available from: DOI: <https://doi.org/10.22038/IJBMS.2019.35125.8353>
- Alhalimi A, Amin S, Beg S, Al-Salahi R, Mir SR, Kohli K. Formulation and optimization of naringin loaded nanostructured lipid carriers using Box-Behnken based design: In vitro and ex vivo evaluation. *J Drug Deliv Sci Technol.* 2022;74(June):103590. Available from: DOI: <https://doi.org/10.3390/pharmaceutics14091771>
- Aggarwal V, Tuli HS, Thakral F, Singhal P, Aggarwal D, Srivastava S, et al. Molecular mechanisms of action of hesperidin in cancer: Recent trends and advancements. *Exp Biol Med.* 2020;245(5):486–97. Available from: DOI: <https://doi.org/10.1177/1535370220903671>
- Saleh N, Allam T, Korany RMS, Abdelfattah AM, Omran AM, Abd Eldaim MA, et al. Protective and Therapeutic Efficacy of Hesperidin versus Cisplatin against Ehrlich Ascites Carcinoma-Induced Renal Damage in Mice. *Pharmaceutics.* 2022;15(3):294. Available from: DOI: <https://doi.org/10.3390/ph15030294>
- Sulaiman GM, Waheeb HM, Jabir MS, Khazaal SH, Dewir YH, Naidoo Y. Hesperidin Loaded on Gold Nanoparticles as a Drug Delivery System for a Successful Biocompatible, Anti-Cancer, Anti-Inflammatory and Phagocytosis Inducer Model. *Sci Rep.* 2020;10(1):1–16. Available from: DOI: <https://doi.org/10.1038/s41598-020-66419-6>
- Martins S, Sarmiento B, Ferreira DC, Souto EB. Lipid-based colloidal carriers for peptide and protein delivery - Liposomes versus lipid nanoparticles. *Int J Nanomedicine.* 2007;2(4):595–607. Available from: <https://pubmed.ncbi.nlm.nih.gov/18203427/>
- Russo E, Spallarossa A, Tasso B, Villa C, Brullo C. Nanotechnology of tyrosine kinase inhibitors in cancer therapy: A perspective. *Int J Mol Sci.* 2021;22(12):6538. Available from: DOI: <https://doi.org/10.3390/ijms22126538>
- Emad NA, Ahmed B, Alhalimi A, Alzobaidi N, Al-Kubati SS. Recent progress in nanocarriers for direct nose to brain drug delivery. *J Drug Deliv Sci Technol.* 2021;64:102642. Available from: DOI: <https://doi.org/10.1016/J.JDDST.2021.102642>
- Vandghanooni S, Rasoulani F, Eskandani M, Akbari Nakhjavani S, Eskandani M. Acriflavine-loaded solid lipid nanoparticles: preparation, physicochemical characterization, and anti-proliferative properties. *Pharm Dev Technol.* 2021;26(9):934–42. Available from: DOI: <https://doi.org/10.1080/10837450.2021.1963276>
- Gupta MK, Swarnkar SK. Preformulation Studies of Diltiazem Hydrochloride from Tableted Microspheres. *J Drug Deliv Ther.* 2018;8(1):64–9. Available from: DOI: <https://doi.org/10.22270/jddt.v8i1.1552>
- Khunteta A, Gupta MK, Swarnkar SK. Formulation of Rapid Dissolving Films Containing Granisetron Hydrochloride and Ondansetron Hydrochloride. *J Drug Deliv Ther.* 2019;9(4-A):516–27. Available from: DOI: <https://doi.org/10.22270/jddt.v9i4-A.3525>
- Mudgil M, Gupta N, Nagpal M, Pawar P. Nanotechnology: A new

- approach for ocular drug delivery system. *International Journal of Pharmacy and Pharmaceutical Sciences*. 2012; 4(2): 105-12.
28. Jain S, Jain S, Khare P, Gulbake A, Bansal D, Jain SK. Design and development of solid lipid nanoparticles for topical delivery of an anti-fungal agent. *Drug Deliv*. 2010;17(6):443–51. Available from: DOI: <https://doi.org/10.3109/10717544.2010.483252>
29. Khunteta A, Gupta MK, Swarnkar SK. Formulation of Rapid Dissolving Films Containing Granisetron Hydrochloride and Ondansetron Hydrochloride. *J Drug Deliv Ther*. 2019;9(4-A):516–27. Available from: DOI: <https://doi.org/10.22270/jddt.v9i4-A.3525>
30. Sipos E, Szabó ZI, Rédei E, Szabó P, Sebe I, Zelkó R. Preparation and characterization of nanofibrous sheets for enhanced oral dissolution of nebivolol hydrochloride. *J Pharm Biomed Anal*. 2016;129:224–8. Available from: DOI: <https://doi.org/10.1016/j.jpba.2016.07.004>
31. Szabó P, Daróczy TB, Tóth G, Zelkó R. In vitro and in silico investigation of electrospun terbinafine hydrochloride-loaded buccal nanofibrous sheets. *J Pharm Biomed Anal*. 2016;131:156–9. Available from: DOI: <https://doi.org/10.1016/j.jpba.2016.08.021>
32. Wong CY, Al-Salami H, Dass CR. The role of chitosan on oral delivery of peptide-loaded nanoparticle formulation. *J Drug Target*. 2018;26(7):551–62. Available from: DOI: <https://doi.org/10.1080/1061186X.2017.1400552>
33. Younes NF, Abdel-Halim SA, Ellassasy AI. Corneal targeted Sertaconazole nitrate loaded cubosomes: Preparation, statistical optimization, in vitro characterization, ex vivo permeation and in vivo studies. *Int J Pharm*. 2018;553(1–2):386–97. Available from: DOI: <https://doi.org/10.1016/j.ijpharm.2018.10.057>
34. Yang S, Zhang X, Wang Y, Wen C, Wang C, Zhou Z, et al. Development of UPLC-MS/MS Method for Studying the Pharmacokinetic Interaction Between Dasatinib and Posaconazole in Rats. *Drug Des Devel Ther*. 2021;15:2171–8. Available from: DOI: <https://doi.org/10.2147/DDDT.S301241>
35. Dheer R, Swarnkar SK, Syeed F. Chromatographic Analysis of *Barleria prionitis* Linn. *Res J Pharm Tech*. 2019;12(8):3679–3686. Available from: DOI: <https://doi.org/10.5958/0974-360X.2019.00628.0>
36. Laxane SN, Swarnkar SK, Setty MM. Antioxidant studies on the ethanolic extract of *Zornia gibbosa*. *Pharmacologyonline*. 2008;1(1):319–30. Available from: https://pharmacologyonline.silae.it/files/archives/2008/vol1/32_Setty.pdf
37. zur Mühlen A, Schwarz C, Mehnert W. Solid lipid nanoparticles (SLN) for controlled drug delivery – Drug release and release mechanism. *Eur J Pharm Biopharm*. 1998;45(2):149–55. Available from: DOI: [https://doi.org/10.1016/s0939-6411\(97\)00150-1](https://doi.org/10.1016/s0939-6411(97)00150-1)
38. Ahmad S, Khan I, Pandit J, Emad NA, Bano S, Dar KI, et al. Brain targeted delivery of carmustine using chitosan coated nanoparticles via nasal route for glioblastoma treatment. *Int J Biol Macromol*. 2022;221:435–45. Available from: DOI: <https://doi.org/10.1016/j.ijbiomac.2022.08.210>
39. Núñez-Sánchez MÁ, Martínez-Sánchez MA, Verdejo-Sánchez M, García-Ibáñez P, Oliva Bolarin A, Ramos-Molina B, et al. Anti-Leukemic Activity of Brassica-Derived Bioactive Compounds in HL-60 Myeloid Leukemia Cells. *Int J Mol Sci*. 2022 2;23(21):13400. Available from: DOI: <https://doi.org/10.3390/ijms232113400>
40. Varshosaz J, Ghaffari S, Khoshayand MR, Atyabi F, Azarmi S, Kobarfard F. Development and optimization of solid lipid nanoparticles of amikacin by central composite design. *J Liposome Res*. 2010;20(2):97–104. Available from: DOI: <https://doi.org/10.3109/08982100903103904>
41. Manda H, Swarnkar SK, Swarnkar A, Rasal AS, Shanbhag R, Kutty NG. Wound Healing Potential of Pyrazole Derivative. *Pharmacologyonline*. 2009;2(1):53–60. Available from: <https://pharmacologyonline.silae.it/files/newsletter/2009/vol2/7.Manda.pdf>
42. Jain P, Jain S, Swarnkar SK, Sharma S, Paliwal S. Screening of analgesic activity of *Phoenix sylvestris* leaves in rodents. *J Ayurvedic Herb Med*. 2018;4(1):22–4. Available from: https://www.ayurvedjournal.com/JAHM_201841_05.pdf
43. Swarnkar S, Jain Y, Kumawat M, Khunteta A, Paliwal S. Exploration of autonomic involvement in mechanism of antinociceptive activity of flowering top extract of *Aerva javanica*. *Asian J Biochem Pharm Res*. 2019;(SI):33–6.
44. Hassan H, Adam SK, Alias E, Meor Mohd Affandi MMR, Shamsuddin AF, Basir R. Central Composite Design for Formulation and Optimization of Solid Lipid Nanoparticles to Enhance Oral Bioavailability of Acyclovir. *Molecules*. 2021;26(18):5432. Available from: DOI: <https://doi.org/10.3390/molecules26185432>
45. Secrétan PH, Karoui M, Bernard M, Ghermani N, Safta F, Yagoubi N, et al. Photodegradation of aqueous argatroban investigated by LC/MSn : Photoproducts, transformation processes and potential implications. *J Pharm Biomed Anal*. 2016;131:223–32. Available from: DOI: <https://doi.org/10.1016/j.jpba.2016.08.033>
46. Zhao Y, Chang YX, Hu X, Liu CY, Quan LH, Liao YH. Solid lipid nanoparticles for sustained pulmonary delivery of Yuxingcao essential oil: Preparation, characterization and in vivo evaluation. *Int J Pharm*. 2017;516(1–2):364–71. Available from: DOI: <https://doi.org/10.1016/j.ijpharm.2016.11.046>